



LAWRENCE
LIVERMORE
NATIONAL
LABORATORY

LLNL-CONF-761102

ON THE RESULTS OF AN EXPERIMENT WITH A MEGAJOULE CLASS HELICAL FLUX COMPRESSION GENERATOR OPERATING AT ABOVE-NOMINAL LEVELS OF CURRENT AND VOLTAGE STRESS

A. J. Young, A. D. White, J. J. Trueblood, A. W. Lodes, H. K. Loey, R. A. Richardson, A. J. Johnson, D. P. Milhous, A. J. Ferriera, R. D. Speer, E. V. Baluyot, A. Bockman, R. K. Hicks, K. M. Hood, J. B. Javedani, S. D. Leahy, T. T. Leever, G. R. Mease, D. B. Norton, A. M. Pearson, A. CS. Ray, M. E. Tillman, D. H. Herrera, P. Dickson, J. A. Gunderson

November 5, 2018

Megagauss Magnetic Field Generation and Related Topics
Kashiwa, Japan
September 25, 2018 through September 29, 2018

Disclaimer

This document was prepared as an account of work sponsored by an agency of the United States government. Neither the United States government nor Lawrence Livermore National Security, LLC, nor any of their employees makes any warranty, expressed or implied, or assumes any legal liability or responsibility for the accuracy, completeness, or usefulness of any information, apparatus, product, or process disclosed, or represents that its use would not infringe privately owned rights. Reference herein to any specific commercial product, process, or service by trade name, trademark, manufacturer, or otherwise does not necessarily constitute or imply its endorsement, recommendation, or favoring by the United States government or Lawrence Livermore National Security, LLC. The views and opinions of authors expressed herein do not necessarily state or reflect those of the United States government or Lawrence Livermore National Security, LLC, and shall not be used for advertising or product endorsement purposes.

On the Results of an Experiment with a Megajoule Class Helical Flux Compression Generator Operating at Above Nominal Levels of Current and Voltage Stress

A. J. Young, A. D. White, J. J. Trueblood, A. W. Lodes, H. K. Loey, R. A. Richardson, A. J. Johnson, D. P. Milhous, A. J. Ferriera, R. D. Speer, E. V. Baluyot, A. Bockman, R. K. Hicks, K. M. Hood, J. B. Javedani, S. D. Leahy, T. T. Leever, G. R. Mease, D. B. Norton, A. M. Pearson, A. C. S.

Ray, M. E. Tillman

Lawrence Livermore National Laboratory

Livermore, USA

young114@llnl.gov

D. H. Herrera, P. Dickson, J. A. Gunderson

Los Alamos National Laboratory

Los Alamos, USA

Abstract— An experiment conducted with a megajoule class helical flux compression generator (HFCG), operating into a primarily inductive load, is described. The motivation behind the experiment was to benchmark the performance of the generator at higher currents and voltages than were tested in prior experiments. The intention was to push operation into a regime where flux loss was likely to become nonlinear, thereby gaining some insight into performance limitations of the design. Another goal was the desire to benchmark the suite of computational tools used to predict the performance of the design, especially in regimes of nonlinear flux loss. In the experiment, the HFCG was seeded with 105 kA (1.05 Wb), and produced 8.6 MA (0.28 Wb) into the load. This result differed significantly from computational models of the experiment, which predicted greater than 10 MA into the load. While more than one source of flux loss was observed in the waveforms, the dominant source of loss appears to be associated with joule heating and magnetic diffusion, which were found to have the most impact during the latter stages of HFCG operation. Details of the experiment design, setup and execution will be given. Analysis of the captured data, along with comparison of these data with model predictions and past experimental data, will be shown.

Keywords—pulsed power, explosive flux compression generator

I. INTRODUCTION

In early 2010, Lawrence Livermore National Laboratory (LLNL) conducted the first of many experiments with the “Mini-G” or “MG” explosive flux compression generator (FCG) system. The MG platform was designed to produce upwards of 60 MA and 8 MJ into an inductive load [1]. The MG platform is composed of two FCG stages – one helical FCG stage which feeds a coaxial FCG. The helical FCG, which is the focus of this paper, is used to boost the output of a capacitor bank in order to seed the coaxial FCG with 8 MA of current, or roughly 1 MJ. An overview of the helical FCG

design has been given previously in [1].

For all of the experiments conducted with the MG helical generator, the peak output current was kept below 9 MA, which satisfied the goals of the original design [1]. Empirical data have shown that performance and repeatability are stable while operating below 9 MA peak current. Also, the suite of modeling and simulation tools used to predict performance, including CAGEN [2] as well as other custom numerical models, have been in reasonable agreement with the experimental data. In other words, confidence in both the expected performance and in the predictive capability of the models is high when operating within these established “nominal” bounds.

In considering new experiments and new experimental capabilities, it is often necessary to predict helical FCG performance in a regime beyond that which has already been empirically established. In these situations, an analysis is typically carried out using models to form a prediction. Judgement is then applied to determine the level of confidence in the prediction. In the case of pulsed power devices like a helical FCG, this confidence will usually scale with the amount, and pedigree, of physics is built into the model.

As one typically has more confidence in interpolation than extrapolation, an experiment was designed using the MG helical FCG to provide a data point for the generator operating at higher levels of flux and current than in any previous experiment. The experiment also provided an opportunity to benchmark the modeling and simulation tools used for predicting FCG performance in a new operating regime. As will be shown herein, the results of the experiment provided valuable insight into failure modes of the generator, while informing the present limitations of the codes.

This work was performed under the auspices of the U.S. Department of Energy by Lawrence Livermore National Laboratory under Contract DE-AC52-07NA27344.

II. EXPERIMENTAL SETUP

A. Experiment Design

The experiment required two major design decisions: what load to connect to the helical FCG output and at what level of current (flux) to seed the experiment with. Since the goal of the experiment was to “stress” the generator beyond what has been seen in the previous experiments, it was first necessary to define stress as it applies to helical FCGs. Although inherently coupled, one may generally categorize helical FCG stress in two ways.

The first category involves stresses resulting from current flow in the generator. Ohmic heating increases conductor temperature and decreases electrical conductivity, which exacerbates flux loss in multiple ways, including increased energy deposition into the conductors. Decreased electrical conductivity increases the rate of diffusion of the magnetic field into conductors, where it is lost from the compression volume. If heating is extreme enough, phase changes in the state of the conductor material occur, which will amplify the effect of flux loss mechanisms. High current densities on conductors will correspond to high magnetic fields. The Lorentz force (also known as $J \times B$ force or magnetic pressure) resulting from high current densities and magnetic fields can deform conductors and decelerate the armature, which can be detrimental to generator performance. Losses related to current stress tend to be incremental. That is, they gradually (albeit in a nonlinear manner) become worse as current stress increases.

The second category involves stresses related to electric fields within the generator. If the electric fields exceed the dielectric strength of the insulating environment within the FCG, then electrical breakdown will occur. This breakdown occurs either between the armature and stator, or between turns in the stator. The onset and impact of electrical breakdown tends to be more abrupt than losses associated with current stress. In other words, electrical breakdown does not gradually become worse as electric field stress is increased. Rather, a threshold is usually crossed at some level of electric field stress at which breakdown occurs.

To make decisions regarding load design and desired seed current for the experiment, it was first necessary to understand how changing those variables would affect stress within the helical FCG. To facilitate this analysis, simulations were conducted across a parameter space of load inductance and seed current. A method for determining increased current stress was found by comparing peak current from the simulations with the maximum peak current observed in experiments, which has been around 8 MA historically. For example, if the model predicted 10 MA peak current for a given load and seed current, that would correspond to a factor 1.25 increase in current stress above “nominal levels”. A similar prediction for increased electric field stress was calculated by considering flux in the generator. From known values of helical FCG inductance, load inductance and seed current one can determine the amount of flux in the system initially. These values from the simulations were compared against past experimental seed flux levels, which were consistently around 0.8 Wb for MG experiments. In an identical manner as the current stress assessment, the ratio of initial flux in the

simulation to initial flux from past experiments yielded a convenient single-value approximation for increased levels of electric field-related stresses in the system. It was understood that these methods for approximating increased stress were simplistic, but they nonetheless enabled an efficient comparison of options across a relatively large trade space. After the analysis was completed, the load inductance selected for the experiment was 32 nH, while the desired seed current was chosen to be 100 kA. According to model predictions, this combination of load inductance and seed current would produce a similar increase, approximately 1.25-fold, in both current and electrical field stress over prior experiments.

To diagnose FCG performance in the experiment, a suite of magnetic and electric field sensors were integrated into the generator and load. A set of four B-dot probes were placed in the load, along with two fibers for Faraday rotation measurements. Another two fibers were placed near the output of the helical FCG as well. Three D-dot sensors were integrated into a power flow section adjoining the generator and the load. For these measurements, the D-dot sensors were terminated in such a way that the resulting signal would be proportional to voltage at the measurement point rather than the derivative of voltage. Details regarding the implementation of magnetic field sensors in LLNL FCG experiments can be found in [3-5], while a thorough description of the D-dot design and implementation, for this experiment specifically, is given in [6].

B. Experiment Execution

The experiment was conducted at the Los Alamos National Laboratory Ancho Canyon facility, which is where LLNL currently conducts many high explosive pulsed power tests [7]. Initial flux was provided by a 330 μ F capacitor, connected to the experiment via coaxial cables connected in parallel. In this configuration, the quarter period of the discharge was expected to be $\sim 90 \mu$ s. There was some concern that this discharge could affect FCG operation, as other researchers have attributed degraded helical generator performance to stresses occurring during the seed phase of an experiment [8]. To minimize stress in the helical FCG during the seeding phase, it was decided that crowbar of the helical FCG should occur as early as possible in the capacitor discharge pulse. To facilitate this, the capacitor was charged to the maximum allowable voltage, 25 kV, prior to being discharged into the experiment. Timing of the high explosives’ initiation in the generator was then set to cause FCG crowbar to occur on the rising edge of the seed current pulse, at an amplitude of 100 kA. Using this approach, it was expected that the seed phase time could be reduced to 70 μ s. The tradeoff with this approach was that jitter in the capacitor switch and in the FCG high explosives train increased uncertainty of achieving the target seed current, since crowbar would occur on the rising edge of the pulse (where $dI/dt > 0$), as opposed to the peak of the discharge (where $dI/dt \approx 0$). For this experiment, however, it was more desirable to minimize the possible impact of seed phase effects on the results of the experiment than to precisely achieve the target current.

III. RESULTS AND DISCUSSION

A. Experimental Results

The experiment was conducted successfully and yielded 100% data return from all diagnostics. Figures 1 and 2 show current derivative and current, respectively, which were derived from the signals captured from the B-dot and Faraday rotation sensors. For both figures, note that the minor oscillations in the Faraday rotation data are byproducts of signal analysis. These are particularly evident in Fig. 1, where a numerical derivative of the recorded data was taken. It is typically extremely difficult to take the numerical derivative of a recorded signal and make meaningful comparisons with other data (which directly measure the derivative) because either (1) noise in the recorded signal is greatly amplified by taking the derivative, or (2) filtering the signal based on a numerical derivative, because of (1), removes desired information from the waveform as well, with agreement between signals suffering as a result. With the exception of the aforementioned oscillations, both the current and current derivative waveforms, from all of the magnetic field sensors, are in good agreement – showing only a 2% discrepancy at peak current for the sensor-averaged signals. From these data, maximum delivered current into the load was estimated to be 8.6 MA.

Figure 3 shows the voltage across the power flow between the generator and the load, using the signals captured by the three D-dot sensors. Overlaid with these waveforms is a plot of the current derivative signal scaled by the load inductance (i.e. 32 nH). The waveshapes of the processed D-dot signals are in excellent agreement with the scaled current derivative waveform. Agreement between the waveforms leaves room for improvement, with a 13% discrepancy at the waveforms' peak. These data suggest that a peak voltage of approximately 14 kV developed across the input feed to the load.

Using the above data, conventional performance metrics for the helical FCG (i.e current and energy gain, flux

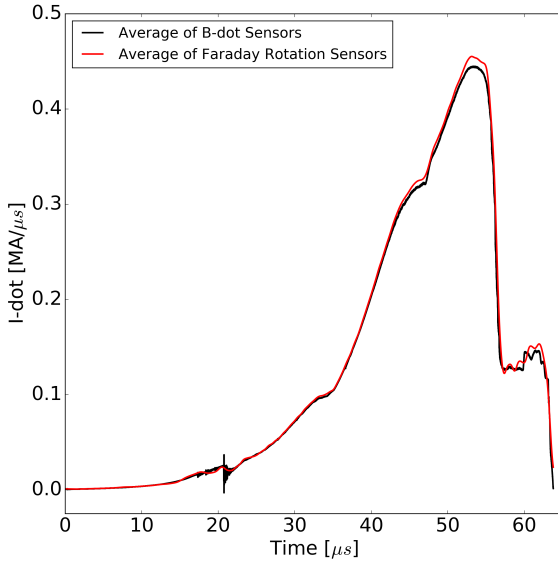


Fig. 1. Overlay of current derivative waveforms taken from B-dot and Faraday rotation sensor signals.

conservation) calculated. The current at the time of FCG crowbar was 105 kA, slightly higher than the original target value. The peak current in the generator was 8.6 MA, which gives an FCG current gain of 82. In terms of energy, the generator was seeded with 55 kJ, and produced a maximum of 1.2 MJ in the load, leading to an energy gain of 22. From the flux perspective, the system was seeded with 1.05 Wb, and there were 0.28 Wb remaining at FCG burnout, resulting in only 27% flux conservation.

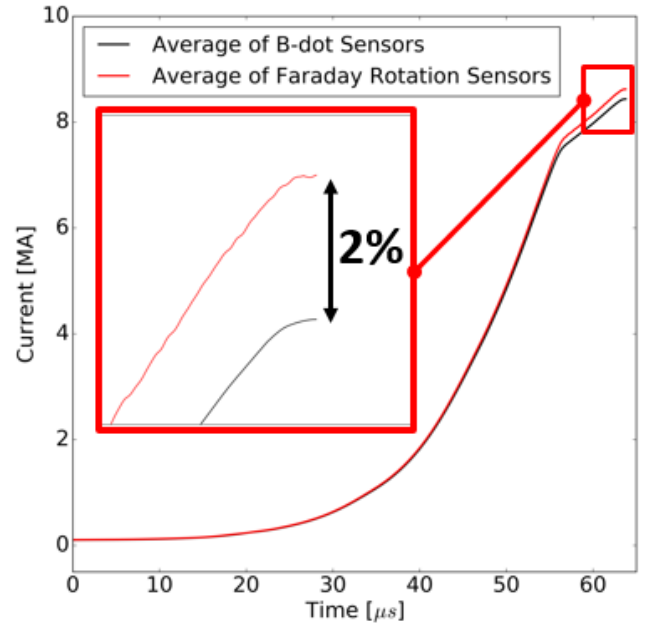


Fig. 2. Overlay of current waveforms taken from B-dot and Faraday rotation sensor signals.

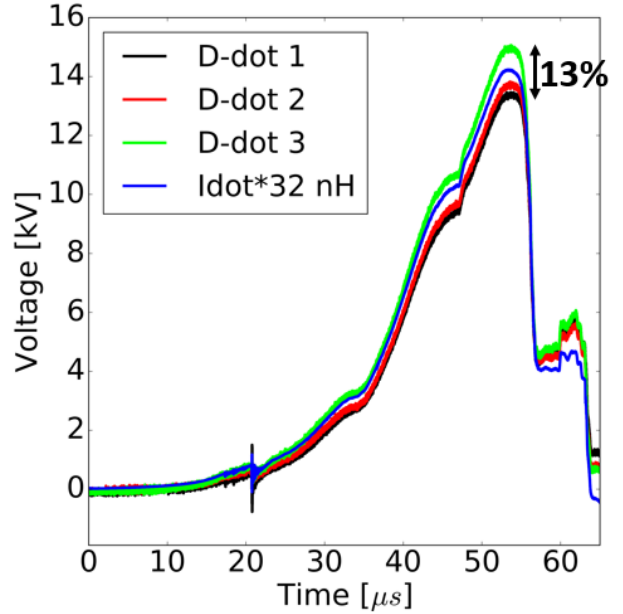


Fig. 3. Overlay of processed D-dot signals along with a current derivative waveform scaled by the load inductance.

B. Post Experiment Analysis

The first assessment to be made after processing the data was to determine how successful the experiment was in stressing the helical FCG. By only examining peak current, one might assume that the generator was not stressed significantly as compared to prior experiments (8.6 MA for this experiment versus 8 MA for prior experiments). However, it was known that the helical generator was seeded with 1.3 times more current than in past experiments, so obviously the amount of current stress varied in time. Figure 4 shows an overlay of the

TABLE I.

	$t = 0 \mu s$	$t = 15 \mu s$	$t = 30 \mu s$	$t = 45 \mu s$	$t = 65 \mu s$
$I_{\text{Experiment}}$	105 kA	154 kA	630 kA	3.1 MA	8.6 MA
I_{MG}	80 kA	123 kA	494 kA	2.3 MA	8.0 MA
$\Phi_{\text{Experiment}}$	1.05 Wb	0.99 Wb	0.80 Wb	0.52 Wb	0.28 Wb
Φ_{MG}	0.81 Wb	0.80 Wb	0.65 Wb	0.47 Wb	0.36 Wb

current derivative waveform from this experiment with the current derivative from a prior MG experiment. What is clear from inspection of these waveforms is that the current derivative is greater in this experiment than in prior experiments for a majority of generator operation. It should be noted that the differences in late time current derivative are expected. Recall that in prior MG experiments, the helical generator served as an intermediate booster between the capacitor bank and the coaxial FCG. As the helical generator approaches burnout, the coaxial generator has also started functioning, and so flux in the system continues to be compressed (at a faster rate) – hence the increase in current derivative. In this experiment, the load is static, and therefore the current derivative is governed by the collapsing inductance of the helical FCG only. The rate of flux compression, and with it the current derivative, go to zero at generator burnout. Table

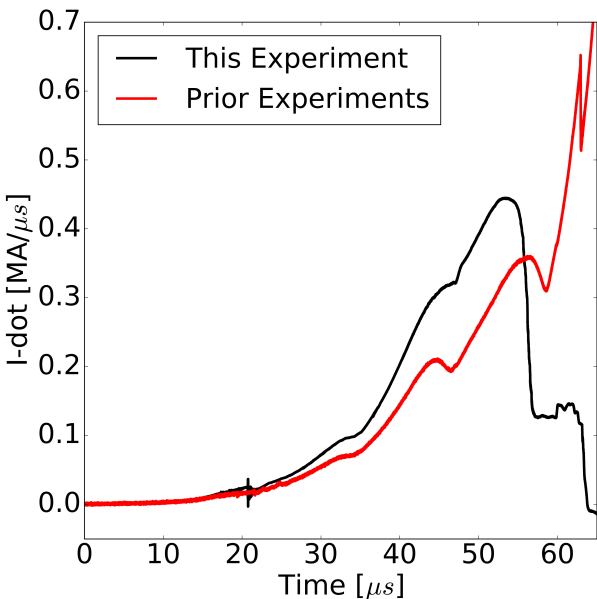


Fig. 4. Overlay of current derivative waveforms from this experiment and from prior MG experiments.

I provides a summary comparison between current and flux, for this experiment and nominal MG experiments, at a few snapshots in time. From the table, it can be seen that the current in this experiment was at least a factor of 1.2 greater than previous MG experiments for a majority of generator operation. At generator burnout the current was a factor of 1.1 greater. Seeding the experiment with 1.05 Wb translated to a factor of 1.3 increase over MG tests. However, by generator burnout, the amount of flux in the system, 0.28 Wb, was lower than the amount of flux in a MG experiment, by about 22%. Table I shows that, for a significant percentage of generator operation, the flux (and therefore electric field stress) was also greater in this experiment than in prior experiments.

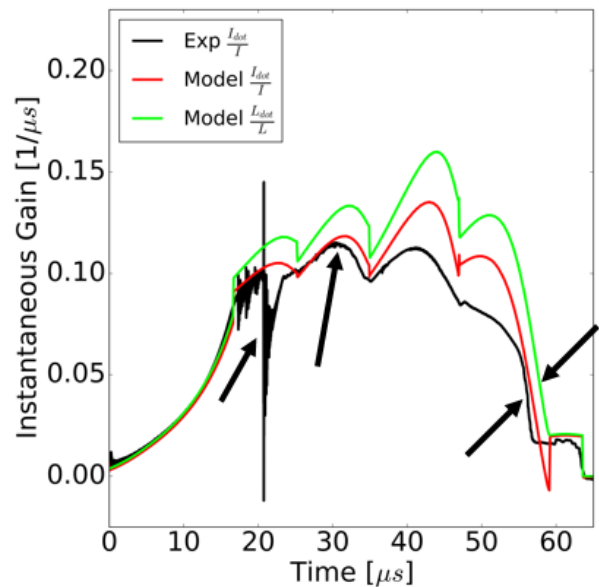


Fig. 5. Overlay of instantaneous gain waveforms, as calculated from the experimental data and a pre-experiment model. Arrows indicate deviations, or the onset thereof, between the model and the data.

Immediately after processing the data, it was obvious that the pre-experiment models had overpredicted the performance of the FCG by a significant margin. Figure 5 shows an overlay of instantaneous gain in the helical FCG versus time, for both the experiment and pre-experiment model. For the experiment, the instantaneous gain is determined by dividing the current derivative by the current. For the model, the instantaneous gain is shown in two different ways. The first is using the same method as the experiment, that is by dividing current derivative by the current. This takes into account the losses as calculated by the model. The second portrayal of instantaneous gain is derived by dividing the inductance derivative by the inductance. This conveys the ideal instantaneous gain of the model, and provides a “lossless” gain comparison with the experimental data. A comparison of the simulation and experimental data shows that several mechanisms of flux loss affected FCG performance, and these losses were not completely captured by the model.

The first flux loss event occurs at approximately 20 μs , see Fig. 5, when the armature was phasing through the first winding section of the coil. Of the possible causes, the

abruptness in onset of the event combined with its short duration was suggestive of electrical breakdown. Flux loss resulting from breakdown would not be captured by the models at present, although it is an active area of research by others [9]. For this experiment, analysis indicates that only 5% of the initial flux was lost during the breakdown event, and therefore considered to be non-catastrophic. A microsecond or two after the onset of the breakdown, it is quenched, and nominal operation resumes for a time, as evidenced by the agreement between the waveforms in Fig. 5.

At about 30 μ s (see Fig. 5), at which point the armature is phasing through the second winding section, the gain in the experiment begins to diverge from the gain in the model. This divergence persists, and grows, through the remainder of generator operation. The fact that the divergence is not abrupt, rather it becomes worse over time is suggestive of flux loss related to current stress. Analysis to this point has not provided a clear indication as to the exact mechanism of loss while the armature is phasing through the second and third winding sections of the coil. Since the phasing time of the armature through the winding sections in the model is consistent with the experimental data until the fourth winding section, one hypothesis is that electrical conductivity-related losses may be mostly responsible. However, analysis using magneto-hydrodynamic (MHD) codes has indicated that mechanical stress, i.e. coil deformation and armature deceleration, had a significant impact on generator function in the fourth winding section, and possibly earlier. Coil deformation is not accounted for in the numerical models presented here, and thus it is possible that magnetic pressure induced flux loss explains the discrepancy between the data and the simulations. Ongoing analysis is focused on understanding flux loss during this experiment using MHD codes. A better understanding of flux loss would be used to drive changes to the numerical models, with the intent of improving predictive capability.

IV. CONCLUSIONS

In summary, an experiment was designed and executed to test a megajoule class helical FCG at higher levels of stress than had been reached in prior experiments. The data captured from the experiment was also used benchmark numerical models in regimes where nonlinear losses significantly affect generator performance.

In the experiment, the 105 kA of seed current was delivered to the generator, which exceeded prior tests by a factor 1.3. While the peak current, 8.6 MA, was only a factor 1.1 greater than historical data, analysis showed that on average current through the helical FCG during operation was greater than a factor of 1.2. Initial flux in the generator, 1.05 Wb, was 1.3 times previous seed flux levels. At generator burnout, 0.28 Wb had been compressed into the load. Although this value of flux

is less than what remains in MG experiments (0.36 Wb), analysis indicates that more flux (in comparison to a MG experiment) was present in the experiment until late in time.

Comparisons of the experimental data with historical data and pre-experiment models indicated that generator performance was degraded by multiple flux loss mechanisms. An abrupt loss early in generator function, attributed to electrical breakdown, was short lived and only resulted in 5% loss of flux. Nonlinear losses affected performance as early as the second winding section and became more detrimental as the FCG approached burnout. Standard modeling approaches were optimistic in their prediction of helical FCG performance, and comparisons with the data exposed a failure of the models to capture significant loss, starting as early as the second winding section. Ongoing work is focused on MHD analyses of the experiment to gain a better understanding of generator performance and to help explain discrepancies between the observed performance and pre-experiment models.

REFERENCES

- [1] D.B. Reisman, J.B. Javedani, et al., "Explosive Flux Compression Generators at LLNL," Proceedings of the 14th International Conference on Megagauss Field Generation and Related Topics, 2012.
- [2] J.B. Chase, D. Chato, G. Peterson, P. Pincosy, G.F. Kiutu, "CAGE N: a Modern, PC Based Modeling Tool for Explosive MCG Generators and Attached Loads," Proceedings of the 12th IEEE International Pulsed Power Conference, 1999, pp.597-600.
- [3] D.A. Goerz, R.A. Anderson, A.D. White, J.B. Javedani, D.B. Reisman, T.J. Ferriera, E.V. Baluyot, R.D. Speer, D.P. Milhous, "Implementation of Pulsed Power Diagnostics of Explosive Flux Compression Generators at LLNL," Proceedings of the 13th International Conference on Megagauss Magnetic Field Generation and Related Topics, 2010.
- [4] A.D. White, G.B. McHale, D.A. Goerz, "Advances in Optical Fiber-Based Faraday Rotation Diagnostics," Proceedings of the 17th IEEE International Pulsed Power Conference, 2009, pp.1358-1363.
- [5] A.D. White, R.A. Anderson, T.J. Ferriera, D.A. Goerz, "Frequency-Domain Methods for Characterization of Pulsed Power Diagnostics," Proceedings of the 17th IEEE International Pulsed Power Conference, 2009, pp.1364-1367.
- [6] R.A. Richardson, A.J. Johnson, A.D. White, J.J. Trueblood, J.B. Javedani, D.P. Milhous, T.J. Ferriera, "A Small D-dot Sensor for use on Flux Compression Generators," *these proceedings*.
- [7] A.J. Young, et al., "LLNL High Explosive Pulsed Power Capabilities and Experiments at the Ancho Canyon Test Site," Proceedings of the 15th International Conference on Megagauss Magnetic Field Generation and Related Topics, 2016.
- [8] J.H. Goforth, H.S. Caird, C.M. Fowler, A.E. Greene, H.W. Kruse, I.R. Lindemuth, H. Oona, R.E. Reinovsky, "Performance of the Laguna Pulsed Power System," Proceedings of the 6th International Pulsed Power Conference, 1987.
- [9] G.F. Kiutu, J.B. Chase, J.B. Javedani, "Electric Field and Breakdown Modeling of Helical Explosive Generators," *these proceedings*.